Tetrahedron 66 (2010) 6101–6112

Contents lists available at ScienceDirect

Tetrahedron

journal homepage: www.elsevier.com/locate/tet

# H-Bonded metallomesogens derived from salicyladiminates

Sih-Yeh Li [a], Chun-Jung Chen [a], Po-Yuan Lo [b], Hwo-Shuenn Sheu [c], Gene-Hsiang Lee [d], Chung K. Lai [a,*]

[a] Department of Chemistry, National Central University, Chung-Li 32001, Taiwan, ROC
[b] Industrial Technology Research Institute, Hsinchu 300, Taiwan, ROC
[c] National Synchrotron Radiation Research Center, Hsinchu 30077, Taiwan, ROC
[d] Instrumentation Center, National Taiwan University, Taipei 10660, Taiwan, ROC

ARTICLE INFO

*Article history:*
Received 19 April 2010
Received in revised form 26 May 2010
Accepted 1 June 2010
Available online 12 June 2010

ABSTRACT

A series of new mesogenic compounds **1a**–**b** ($n$=8, 10, 12, 14, 16) derived from salicyladimines and their palladium **2a**, **2b**, vanadyl **2a**, and copper complexes **3a**, **3b** were prepared and their mesomorphic properties investigated by optical microscopy, differential scanning calorimetry and powder X-ray diffractometry. $Pd^{2+}$ and $VO^{2+}$ ions formed *mononuclear complexes*, whereas, $Cu^{2+}$ ion formed *binuclear* complexes due to the relative acidic strength of Schiff base. Single crystallographic analysis of non-mesogenic compound **2a** ($n$=8) confirmed its coordination geometry at $Pd^{2+}$ as square plane. It crystallizes in a triclinic space group $P\bar{1}$ with a Z=1. As expected, the $Pd^{2+}$ was coordinated via a *trans*-$N_2O_2$ donor set of phenolic–O and imine-N atoms, leaving two hydroxyl groups intact and uncoordinated. The two alkoxy chains, pointing to the opposite direction were parallel, and the molecule was considered as twisted Z-shaped. Both hydroxyl-OH groups attached on $C_{17}$ and $C_{18}$-Schiff imines participate in the H-bonds in the lattice. Interestingly, a pseudo polymeric structure was observed, in which H-bonded dimer was continuously extended by another H-bonded dimer in the lattice. Compounds **1** exhibited smectic A phases, and Pd and VO complexes and Cu complexes **3b** exhibited smectic A or/and smectic X phases, however, Cu complexes **3a** formed crystal phases. Intermolecular H-bonds might be attributed to the difference observed on the mesomorphic properties in these compounds. Copper complexes **2b** were not active on ESR spectroscopy.



## 1. Introduction

The use of intermolecular attraction induced (or stabilized) by hydrogen-bonds to generate organic mesogenic materials has been well demonstrated during the past years. The approach by H-bonding allowed us to tailor molecular engineering for functional organic liquid crystals. Numerous novel examples[1] prompted by either intermolecular or/and intramolecular were described, in which both using single component or multiple components were all accessible. There is often a competition between inter-molecular and intra-molecular H-bonding. In order to achieve a stable mesogenic state, a balance between the tendency of the molecules to melt or to segregate into a crystalline state becomes crucially important. H-bond interaction; considered as a relatively weak force might not be the principle attraction in forming the mesophase. Other interactions, as well as π–π interaction, weal dipole, van der Waals force and others might be concomitant. In contrast, metallomesogenic materials[2] approached by same concept were relatively limited. The presence of one or more hydroxyl groups in the organic moiety is truly compulsory in order to induce such attractive H-bonds. Likewise, the hydroxyl groups were also an excellent coordination sites toward most of transition metals, thus leaving no free hydroxyl group to be induced in mesogenic states. Diamagnetic palladium ($d^8$-$Pd^{2+}$) and paramagnetic oxovanadium or vanadyl ($d^1$-$V^{IV}O^{2+}$) ions were considered exclusively as a few metal ions. $Pd^{2+}$ ion is often considered as soft Lewis acid, whereas, $VO^{2+}$ is then regarded as harder Lewis acid. These two metal ions will not coordinate to the hydroxyl groups with a less acidic strength, particularly to the primary-OH (1°), and secondary-OH (2°) of the alkyl alcohols. However, they do coordinate to the phenolic hydroxyl group.

Recently, we have been interested in this type of stabilized H-bonded metallomesogens, and a few H-bonded metallomesogens **4**,[3] **5**[4] have been prepared and reported by this group. Complexes **4** formed smectic A phases, however, complexes **5** exhibited hexagonal columnar phases. Interestingly, single crystallographic analysis indicated that a dimeric structure

* Corresponding author. Tel.: +886 03 4259207; fax: +886 03 4277972; e-mail address: cklai@cc.ncu.edu.tw (C.K. Lai).

0040-4020/$ – see front matter © 2010 Elsevier Ltd. All rights reserved.
doi:10.1016/j.tet.2010.06.002

in compounds **4** and a tetrameric structure in compound **5** by H-bond were observed in the crystal states, and the formation of mesophases induced might be attributed to such H-bond in the mesophases. A smectic A phase and hexagonal phase was observed by H-bonded dimeric and tetrameric structure for compounds **1** and **4**, respectively. An appropriate aspect ratio or/and resulting complementary shape effect were probably improved by H-bonds. A removal of hydroxyl group then led to the loss of liquid crystallinity in both complexes. In addition, the position (or location) of the hydroxyl groups has a significant impact on the liquid crystalline behavior; changing their position often dramatically alters their geometries needed to induce the H-bond interactions. Salicyladimine Schiff bases are one of the organic moieties that have been studied the most, and many mesogenic palladium complexes[5] were reported. Interestingly, a series of mononuclear copper(II) complex[6] derived from azo-containing salicylaldimines was prepared and studied by Rezvani and co-workers. A free hydroxyl group on ethanolamine Schiff base was remained as uncoordinated, however, whether H-bond existing was uncertain due to the lack of single crystallographic analysis.

In this work, a new series of mesogenic compounds **1** ($n$=8, 10, 12, 14, 16) derived from salicyladimines and their palladium, vanadyl, and copper complexes **2**, **3** were prepared and their mesomorphic properties studied. Single crystallographic analysis of non-mesogenic compound **2a** ($n$=8) confirmed the square planar geometry at $Pd^{2+}$ center, and also a pseudo-polymeric structure induced by intermolecular H-bonds were formed. Both hydroxyl-OH groups are important since they all participate in the H-bonds in the crystal lattice. Palladium **2a**, **2b** and vanadyl complexes **2a** are mononuclear complexes; however, copper complexes **3a**, **3b** are binuclear complexes. A structurally similar bimetallomesogens **6**[7a,b], **7**[7c] were also reported by this group. Single crystallographic data indicated that these copper complexes were all dinuclear coordinated with one copper atom lying above and below the central plane.

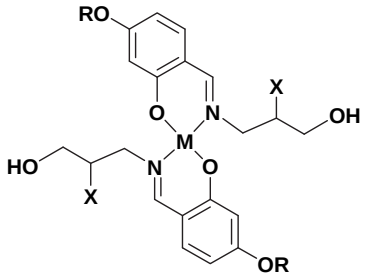


**M = Pd, VO; R = $(CH_2)_nH$**
**2a; X = OH**
**2b; X = H**

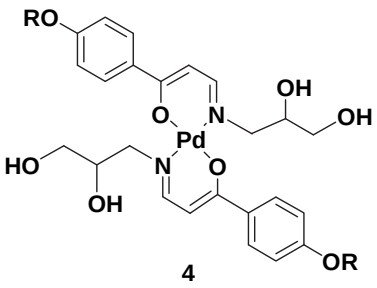


**4**

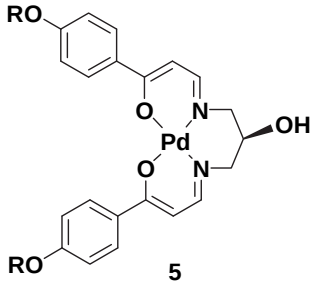


**5**

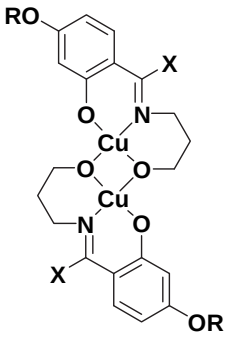


**6; X = H, $CH_3$**

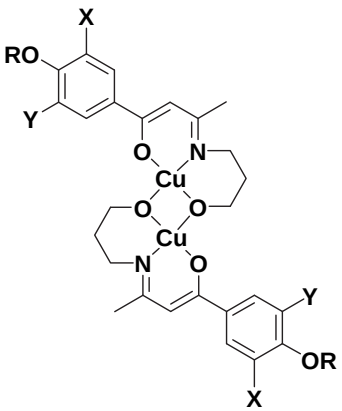


**7; X, Y = H, OR**

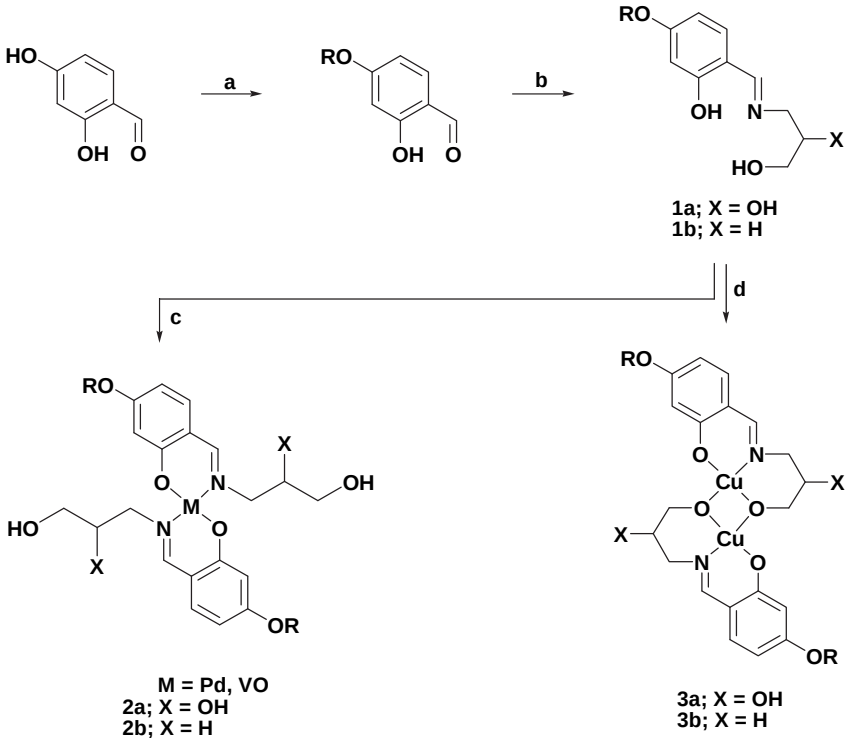


**Scheme 1.** Reactions and reagents. (a) $KHCO_3$ (2.0 equiv), KI, RBr (1.1 equiv), refluxing in acetone, 16 h, 40%. (b) 3-Amino-propane-1,2-diol (1.1 equiv) or 3-amino-propanol (1.1 equiv), refluxing in THF/absolute ethanol, 3 h, 90%. (c) $M(OAC)_2$ (M=Pd, VO; 0.55 equiv), refluxing in $C_2H_5OH$, 6 h. 75%. (d) $Cu(OAC)_2$ (1.1 equiv), refluxing in ethanol, 6 h, 80%.

## 2. Results and discussion

### 2.1. Synthesis and characterization

The synthetic pathways to compounds **1a**, **1b** and their palladium(II) **2a**, **2b**, vanadyl **2a** and copper(II) complexes **3a**, **3b** are summarized in Scheme 1. All intermediates and Schiff bases were characterizes by $^1H$ and $^{13}C$ NMR spectroscopy. A characteristic peak appeared at ca. $\delta$ 8.02–8.13, assigned for an imine-H (−C═N*H*) of compounds **1a**, **1b** was observed. Metal complexes **2**, **3**, prepared by the reactions of Schiff bases **1** with vanadyl(IV) sulfate, palladium(II) acetate or copper acetate refluxing in ethanol were obtained after recrystallization twice from THF/methanol. All palladium and vanadyl complexes were isolated as yellow and gray-green solids; however, all binuclear copper complexes were obtained as pale green solids. These bicopper $d^9$-$[Cu^{2+}]_2$ complexes

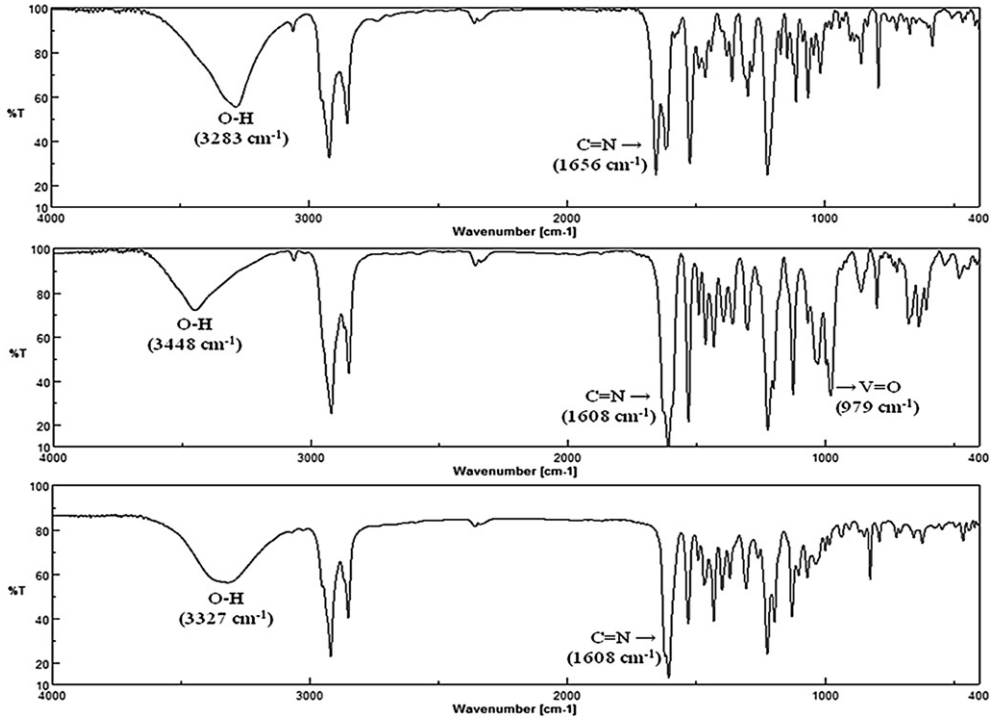


**Figure 1.** The IR spectra measured at 25.0 °C of the compounds: **1a** ($n$=10; top), VO complex **2a** ($n$=10) and Pd complex **2a** ($n$=10; bottom).

**3a**, **3b** and monovanadyl $d^1$-$V^{IV}O^{2+}$ **2a** are all paramagnetic, and their $^1$H NMR spectra displayed only one broad alkoxy signals. All other proton signals close to paramagnetic metal center were not all well observed. In addition, these paramagnetic $d^9$-$[Cu^{2+}]_2$ complexes showed no signal at 77 K and 298 K on solid-samples EPS spectroscopy due to the super exchange behavior.

The IR spectral frequencies of a few compounds **1a** ($n$=10) and **2a** (M=VO, Pd; $n$=10) were obtained using KBr pellets. In the compounds **1a** ($n$=10), the imine −C═N and the hydroxyl −OH groups were observed at $\nu_{C=N}$=1656 cm$^{-1}$, and $\nu_{OH}$=3250–3450 cm$^{-1}$, as shown in Figure 1. Upon complexation, the VO complexes **2a** ($n$=10) has a $\nu_{C=N}$ frequency shifted to lower 1608 cm$^{-1}$, and another $\nu_{(V=O)}$ frequency was observed at 979 cm$^{-1}$, indicative of the formation of the mononuclear five-coordinate with square-pyramid geometries.[8] On the other hand, the phenolic −OH group often, occurred at $\nu_{OH}$=3200 cm$^{-1}$ was slightly superimposed with the two lateral −OH groups observed at $\nu_{OH}$=3320 cm$^{-1}$. Infrared data were much less informative for the palladium complexes **2a** (C═N and N═N stretching modes overlapped in the same region). All vanadyl complexes were only slightly soluble in polar solvents; however, they were not quite stable in such solvents. The solution changed to red in color in few minutes when dissolved in THF, and this might be associated to the coordination of THF to the vanadyl center as the sixth ligand. Removal of THF would not lead back to the original structure. In order to evaluate electrochemical properties of the bicopper complex, the cyclic voltammetry (CV) measurements (Fig. 2) were performed in a dry dichloromethane solution of $Bu_4NPF_6$ (0.1 M) with a scan rate of 100 mV s$^{-1}$ at room temperature. Compound **3a** ($n$=16) showed a quasi-reversible peak[9] at −0.65 V and −0.71 V, $E_{1/2}$=0.61 V ($\delta E_P$=65 mV). The one-electron reduction can be ascribed to the oxidation reaction of bicopper complexes as $[(Cu^{2+}Cu^{2+})L]+e^- \leftrightarrow [(Cu^{+}Cu^{2+})L]^-$.

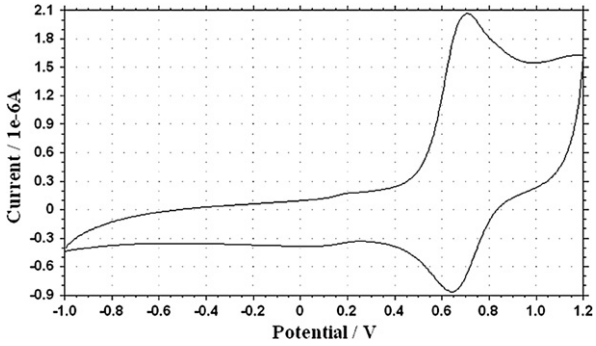


**Figure 2.** Cyclic voltammogram of copper complex **3a** ($n$=16) in $CH_2Cl_2$/0.1 M $Bu_4NPF_6$ at 25 °C.

## 2.2. Single crystal structure of palladium complex of 3-[(2-hydroxy-4-octyloxy benzylidene)amino]propane-1,2-diol (2a; *n*=8)

In order to confirm the geometry at central $Pd^{2+}$ ion, and also understand the possible effect of the two hydroxyl groups (−OH) on the formation of mesophases, a single crystal of the non-mesogenic palladium complex **2a** ($n$=8) suitable for crystallographic analysis was obtained by slow vaporization from THF/methanol at room temperature and it structure resolved. As expected, the palladium ion was coordinated via a *trans*-$N_2O_2$ donor set of phenolic-O and imine-N atoms, leaving the two hydroxyl groups intact and uncoordinated. Figure 3 shows the molecular structure with the atomic numbering schemes. Table 1 lists its crystallographic and structural refinement data. It crystallizes in a triclinic space group $P$−1 with a $Z$=1. The geometry at palladium center is a nearly perfect square

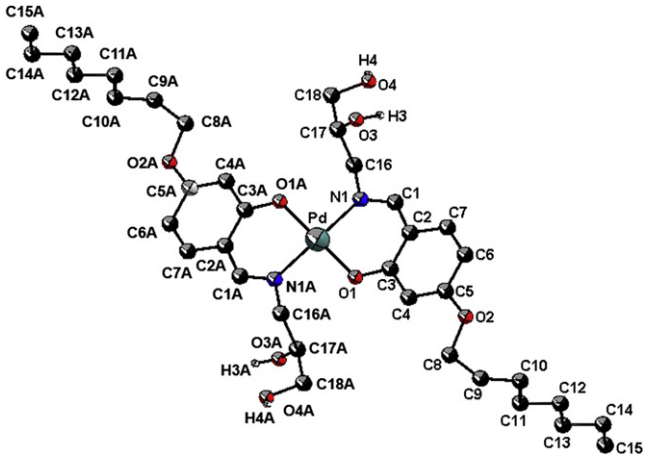


**Figure 3.** An ORTEP plot for compound **2a** ($n$=8) with the numbering scheme, and the thermal ellipsoids of the non-hydrogen atoms are drawn at the 50% probability level.

**Table 1**
Crystallographic and experimental data for compound **2a** ($n$=8)

| Compound | **2a** ($n$=8) |
|---|---|
| Empirical formula | $C_{36}H_{56}N_2O_8Pd$ |
| Formula weight | 751.23 |
| $T$/K | 150 (2) |
| Crystal system | Triclinic |
| Space group | $P$−1 |
| $a$/Å | 5.3975 (2) |
| $b$/Å | 9.5122 (4) |
| $c$/Å | 17.8000 (4) |
| $\alpha$/° | 78.796 (2) |
| $\beta$/° | 88.670 (3) |
| $\gamma$/° | 84.599 (2) |
| $U$/Å$^3$ | 892.48 (5) |
| $Z$ | 1 |
| $F$ (000) | 396 |
| $D_c$/Mg m$^{-3}$ | 1.398 |
| Crystal size/mm$^3$ | 0.32×0.06×0.02 |
| Range for data collection/° | 2.19–25.00 |
| Reflection collected | 9252 |
| Data, restraints, parameters | 3139/0/227 |
| Independent reflection | 3139 [$R$ (int)=0.0671 |
| Final $R1$, $wR2$ | 0.0443, 0.1044 |

plane. The two angles of N1A–Pd–O1A and O1–Pd–N1A are 91.90 (10)° and 88.10 (10)°, respectively, which show an almost ideal angle of 90° as expected for a square planar coordination. The other two angles of N1–Pd–N1A and O1–Pd–O1A were also perfect of 180°. Selected bond distances and angles for compound **2a** ($n$=8) were listed in Table 2.

**Table 2**
Selected bond distances [Å] and angles [°] for compound **2a** ($n$=8)

| | | | |
|---|---|---|---|
| Bond distances | | | |
| N(1)–Pd | 2.022 (3) | C(2)–C(3) | 1.412 (5) |
| O(1)–Pd | 1.983 (2) | C(3)–O(1) | 1.317 (4) |
| C(1)–C(2) | 1.434 (5) | C(16)–C(17) | 1.535 (5) |
| C(1)–N(1) | 1.287 (4) | C(17)–O(3) | 1.322 (7) |
| C(16)–N(1) | 1.471 (4) | C(18)–O(4) | 1.403 (6) |
| Bond angles | | | |
| O(1)–Pd–N(1) | 91.90 (10) | O(1)A–Pd–N(1)A | 91.90 (10) |
| O(1)–Pd–N(1)A | 88.10 (10) | O(1)A–Pd–N(1) | 88.10 (10) |
| C(3)–O(1)–Pd | 126.1 (2) | C(1)–N(1)–Pd | 122.7 (2) |
| N(1)–C(1)–C(2) | 128.2 (3) | O(3)–C(17)–C(18) | 113.6 (4) |
| N(1)–C(16)–C(17) | 112.8 (3) | O(4)–C(18)–C(17) | 108.0 (4) |

Symmetry transformations used to generate equivalent atoms: #1−$x$, −$y$+2, −$z$.

Two phenyl rings were parallel; however, they were not co-planar with the central plane defined by N1–O1–Pd–N1A–O1A atoms. A dihedral angle of 16.03° was measured. The two alkoxy chains were almost perpendicular to the central Pd plane with an angle of ~89.67°. There was no interaction between the neighboring Pd–Pd atoms (*d* ~5.40 Å) and Pd–O atoms (*d* ~4.38 Å). The two chains were parallel (*d* ~3.929 Å) aligned, pointing to the opposite direction (or a trans arrangement). It led to an overall molecular shape considered as a Z-shaped molecule, and the molecular length was ca. ~24.27 Å (C15–C15A). The middle length and side length were 17.0 and 7.7 Å, giving a total possible fully extended molecular length of 17.0+2×7.7 Å=32.4 Å. Unsurprisingly, two types of intermolecular H-bonds formed by two hydroxyl groups attached on $C_{17}$ and $C_{18}$ Schiff imine were in fact observed in the lattice. Both types are intermolecular H-bonds. The first H-bond was induced by two neighboring molecules above-and-below planes; and the second H-bond was formed by two side-by-side molecules. The first H-bond lengths of above-and below molecules were of ~1.828 Å (O4-H4···O3) and the second one was ~2.030 Å (H3A···O4). The two bond angles, ∠O3–H4–O4 and O4-H3–O3 were of 153.97° and 163.90°, respectively. A pseudo dimeric structure formed by H-bond was arranged by a style of cis arrangement (Fig. 4). This dimeric structure was formed by interlocking two molecules via two symmetric H-bonds; one was C18O4···H3AC17A and other one was C17O3H3··· O4AC18A. On the other hand, no π–π interaction between molecules were observed. The H-bonds facilitated the formation of a layer smectic phase observed in compounds **2a** (Fig. 5). This intermolecular H-bond between two dimeric structures has apparently enhanced the molecular interaction between the layers.

### 2.3. Mesomorphic properties

The liquid crystalline behavior of ligands **1a**, **1b**, bicopper complexes **3a**, **3b**, vanadyl, and palladium complexes **2a**, **2b** were characterized and studied by differential scanning calorimetry (DSC) and polarized optical microscope (POM). The phase transitions and thermodynamic data are summarized in Table 3–5. The only derivative **1a** with a shorter chain (*n*=8) exhibited monotropic behavior, whereas all other derivatives **1a** (*n*=10, 12, 14, 16) with longer alkoxy carbon chains showed enantiotropic phases. Under optical microscope they exhibited oily streak textures (Fig. 6) with a large area of homeotropic domains, which was characteristic of a layer smectic A phase expected for the rod-like molecules. The phases were tentatively assigned as smectic A phases based on POM observation. The clearing temperatures were all ranged at $T_{cl}$=124.4 °C (*n*=8)–132.9 °C (*n*=14), while all melting temperatures remained at *T*=119.8 °C (*n*=10)–114.5 °C (*n*=16). On the other hand, the temperature range of mesophase increased slightly with carbon length of alkoxy chains, Δ*T*=20.8 °C (*n*=8)>40.1 °C (*n*=12)>41.7 °C (*n*=16) on cooling process. The transition enthalpies of SmA-to-Iso transitions were relatively small, and also decreased with carbon length, $\Delta H_{SmA\rightarrow I}$=1.87 (*n*=10)~1.87 kJ/mol (*n*=16). In contrast, all derivatives **1b** (*n*=8, 12, 16) formed monotropic behavior. The clearing temperatures were

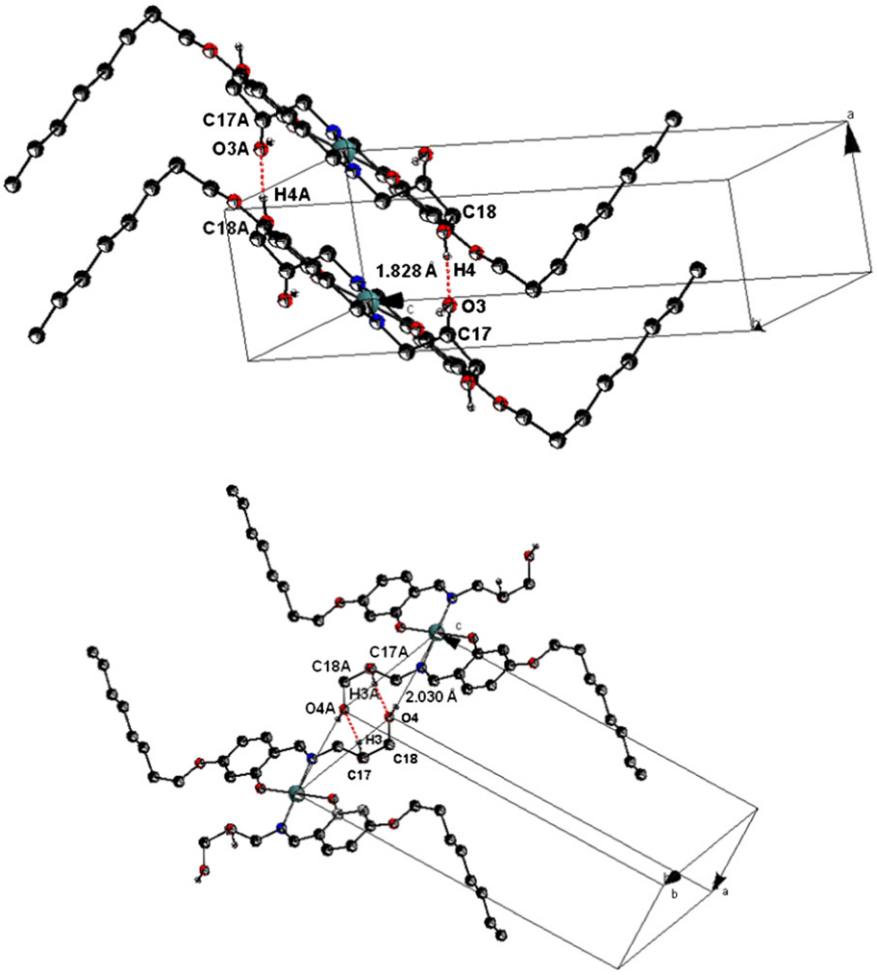


**Figure 4.** Inter-molecular H-bonds in compound **2a** (*n*=8) observed in the unit cell.

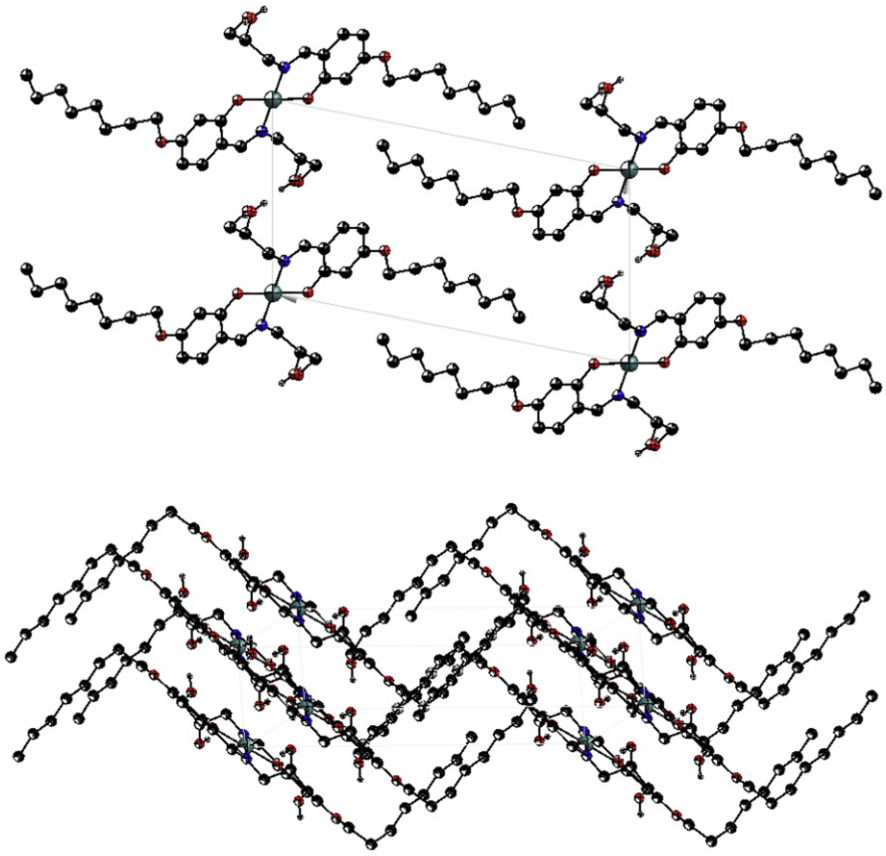

**Figure 5.** The molecular arrangements into layer structures in **2a** ($n$=8) viewed from different axes.

all much lower than those for derivatives **1a** by ca. 82.3 °C ($n$=8)–41.6 °C ($n$=16). However, the temperature range of mesophases for derivative **1b** remained $\Delta T$=9.4 °C ($n$=8)–23.3 °C ($n$=8), slightly narrower than those of derivatives **1a**. The phases were also identified as smectic A phases. A relatively lower enthalpy, $\Delta H$=0.85 ($n$=16)–2.19 kJ/mol ($n$=8) for **1a** and $\Delta H$=3.09 ($n$=8)–3.83 kJ/mol ($n$=12) for **1b** of transition of smectic phase-to-isotropic was also consistent for SmA phases. The difference in the mesomorphic temperatures might be attributed to H-bonds. H-bonding might be induced in both compounds **1a**, **1b**. However, Intermolecular H-bonds induced or/and formed by an extra hydroxyl group at $C_{17}$ in derivatives **1a** have apparently enhanced the intermolecular attraction, leading a higher clearing temperature, and mesophase were also improved.

Palladium complexes derived from **1a**, **1b**, and vanadyl complexes derived from **1a** were also prepared and studied. All Pd compounds, **2a**, **2b** except for those with shorter alkoxy chains ($n$=8) were mesogenic, and both Pd complexes **2a**, **2b** have a much

**Table 3**
Phase temperature and enthalpies[a] of compounds **1a** and **1b**

| | | | | | | | |
|---|---|---|---|---|---|---|---|
| **1a**; n = 8 | | | Cr | | 124.4 (41.8) | | I |
| | | | | 98.7 (29.6) | SmA | 119.5 (2.19) | |
| 10 | $Cr_1$ | 60.7 (19.3) / 58.5 (16.6) | $Cr_2$ | 119.8 (38.1) / 93.3 (29.1) | SmA | 129.6 (1.87) / 128.2 (1.91) | I |
| 12 | $Cr_1$ | 78.0 (25.1) / 68.9 (18.7) | $Cr_2$ | 116.2 (36.4) / 91.4 (30.0) | SmA | 132.9 (1.49) / 131.5 (1.50) | I |
| 14 | $Cr_1$ | 89.6 (31.7) / 75.2 (22.5) | $Cr_2$ | 115.8 (37.5) / 90.6 (30.3) | SmA | 132.9 (1.15) / 131.7 (1.21) | I |
| 16 | $Cr_1$ | 101.8 (36.1) / 78.2 (28.0) | $Cr_2$ | 114.5 (35.2) / 87.5 (28.8) | SmA | 130.6 (0.81) / 129.2 (0.85) | I |
| **1b**; n = 8 | | | Cr | | 42.1 (31.2) | | I |
| | | | | 8.90 (22.8) | SmA | 30.7 (3.09) | |
| 12 | | | Cr | | 79.9 (68.2) | | I |
| | | | | 34.9 (31.9) | SmA | 58.2 (3.83) | |
| 16 | | | Cr | | 89.0 (91.3) | | I |
| | | | | 59.5 (49.1) | SmA | 68.9 (3.81) | |

[a] $n$ is the carbon numbers of terminal alkoxy groups. $Cr_1$, $Cr_2$=crystal, SmA=smectic A, and I=isotropic phase.

**Table 4**
Phase temperatures and enthalpies[a] of compounds **2**

| | | | | | | | | |
|---|---|---|---|---|---|---|---|---|
| **2a**; M = Pd, n = 8 | | | | | | Cr | 192.5 (4.59) / 157.0 (13.3) | I |
| 10 | $Cr_1$ | 155.1 (6.55) / 125.6 (28.5) | $Cr_2$ SmX | 173.4 (17.9) / 150.3 (8.64) | $Cr_3$ SmA | 196.5 (16.0) / 170.8 (3.84) | | I |
| 12 | Cr | 144.5 (29.9) / 123.4 (40.2) | SmX | 169.2 (14.6) / 155.7 (10.4) | SmA | 198.7 (21.8) / 187.2 (5.53) | | I |
| 14 | Cr | 165.3 (4.8) / 121.6 (66.5) | SmX | 196.1 (17.9) / 160.8 (18.3) | SmA | 206.2 (5.70) / 195.2 (6.93) | | I |
| 16 | Cr | 142.6 (70.0) / 118.1 (47.9) | SmX | 193.6 (13.5) / 156.4 (15.2) | SmA | 203.6 (5.39) / 193.3 (6.46) | | I |
| **2a**; M = VO, n = 10 | | | | $Cr_1$ 183.4 (27.8) / 122.7 (6.11) | $Cr_2$ SmA | 194.8 (34.4) / 150.2 (2.20) | | I |
| 12 | | | | $Cr_1$ 165.7 (12.5) / 124.7 (9.12) | $Cr_2$ SmA | 195.4 (37.6) / 168.7 (3.30) | | I |
| 14 | | | | $Cr_1$ 157.7 (10.1) / 127.0 [b] | $Cr_2$ SmA | 196.5 (40.2) / 180.7 (2.65) | | I |
| **2b**; M = Pd, n = 8 | | | | | | Cr | 118.1 (52.7) / 89.5 (46.9) | I |
| 12 | | | | Cr 116.6 (83.3) / 63.1 (87.9) | SmA | 127.8 (3.68) / 124.4 (4.85) | | I |
| 14 | | | | Cr 115.0 (91.2) / 72.2 (99.2) | SmA | 132.3 (3.85) / 128.0 (5.98) | | I |
| 16 | | | | Cr 104.0 (59.8) / 53.9 (61.9) | SmA | 129.5 (4.94) / 127.6 (4.85) | | I |

[a] *n* is the carbon numbers of terminal alkoxy groups. $Cr_1$, $Cr_2$, and $Cr_3$=crystal, SmX=smectic X, SmA=smectic A, and I=isotropic phase.
[b] Obtained by optical microscope.

**Table 5**
Phase temperatures and enthalpies[a] of compounds **3**

| | | | | | | |
|---|---|---|---|---|---|---|
| **3a**; n = 8 | | | Cr | 243.1 (64.1) | | $I_d$ |
| 12 | | | Cr | 229.4 (56.5) | | $I_d$ |
| 16 | | | Cr | 222.1 (56.8) | | $I_d$ |
| **3b**; n = 8 | Cr | 132.4 (27.7) | SmA | 191.4 (25.8) / 137.2 (1.00) | | I |
| 12 | Cr | 127.1 (33.1) | SmA | 171.2 (46.0) / 144.4 (5.15) | | I |
| 16 | Cr | 121.3 (40.4) | SmA | 149.7 (32.1) / 133.9 (7.15) | | I |

[a] *n* is the carbon numbers of terminal alkoxy groups. Cr=crystal, SmA=smectic A, and I=isotropic phase.

higher clearing temperature than those of compounds **1a**, **1b** by a $\Delta T_{cl}$=65.8 °C (*n*=12)–73.3 °C (*n*=14) and $\Delta T_{cl}$=40.5 °C (*n*=16)–76.0 °C (*n*=8), respectively. Likewise, Pd complexes **2a** also have a higher clearing temperature than that of Pd complexes 2**b** by a $\Delta T_{cl}$=70.9 °C (*n*=12)–74.1 °C (*n*=16). This lowering in clearing temperatures observed in **2b** over **2a** might be attributed to the dramatic weakening or loss of H-bonds in Pd complexes **2b**. Compounds **2a** formed smectic X and smectic A phases, however, compounds **2b** formed smectic A phase. An oily streak texture, as characteristic textures of smectic A phases was observed under optical microscope, in which a large area of homeotropic domain was also observed (Fig. 7). Compounds **2a** (*n*=10, 12, 14, 16) have a higher clearing temperature than that of compounds **2b** by ca. $\Delta T_{cl}$=73.9 °C (*n*=14)–81.4 °C (*n*=12). The higher clearing temperatures might be attributed to the H-bond formed by an extra hydroxyl group at $C_{17}$ of Schiff bases. Both series of compounds have a temperature range of mesophase at ca., $\Delta T_{SmA}$=58.4 °C (*n*=10)–74.1 °C (*n*=12) and $\Delta T_{SmA}$=55.8 °C (*n*=14)–73.7 °C (*n*=16) for

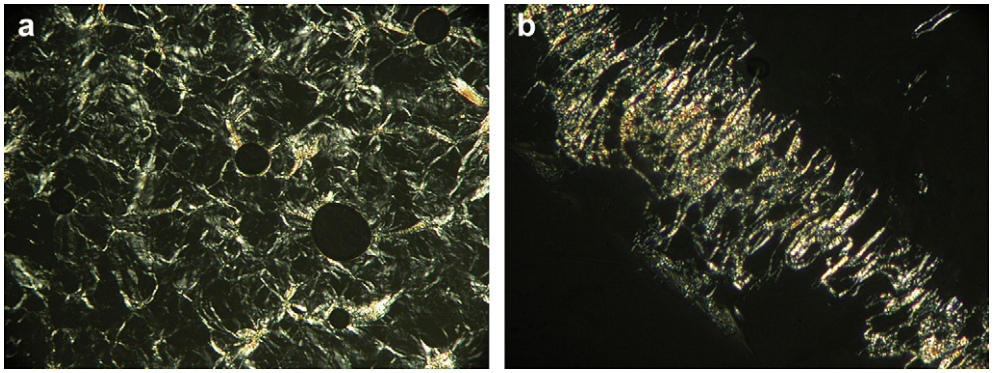


**Figure 6.** The optical textures observed. SmA phase by **1a** (*n*=10; top) at 125.0 °C, SmA phase by **1b** (*n*=8; bottom) at 29.0 °C.

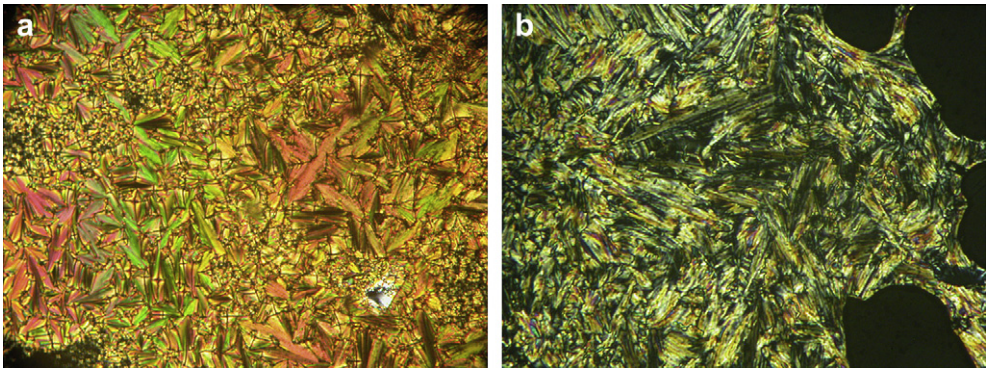


**Figure 7.** The optical textures observed. SmA phase by **2a**/Pd ($n$=10; left) at 192.0 °C and SmX phase by **2a**/Pd ($n$=10; right) at 175.0 °C.

compounds **2a** and **2b**, respectively. An extra highly ordered SmX phase was also observed for compounds **2a** at lower temperatures, of which were not studied further for its phase classification. All VO complexes **2a** ($n$=8, 12, 14, 16) were kinetically unstable in mesophase behavior and they all exhibited monotropic behavior. Compound with a $n$=16 was nonmesogenic. The clearing temperatures were slightly lower than those of Pd complexes by ca. $\Delta T_{cl}$=1.7 ($n$=10)<3.3 ($n$=12)<9.7 °C ($n$=14). The temperature range of mesophase was also slightly narrower by 19.8 ($n$=12)–19.8 °C ($n$=14) that those of Pd complexes **2a**. The mesophase were also assigned as SmA phases based on POM textures.

The bicopper complexes **3a**, **3b** with a central bridging oxygen were also prepared and studied. A structurally similar copper complexes derived from 4-alkoxy-*N*-(3-hydroxypropyl) salicylaldimines and 3,5-bis-(3,4,5-trialkoxybenzyloxy)phenyl-2-(3-hydroxypropyl)imino propylketones **6**, **7** have been prepared and investigated in this group. The geometry of these bicopper complexes was perfectly square pyramid, in which two copper atoms were found lying 3.0375 (5) Å apart, one 0.018 Å above and the other 0.018 Å. The center core was nearly flat, which facilitated the molecular arrangement. Copper complexes have a relatively larger core size, so a higher clearing temperature might be expected. From

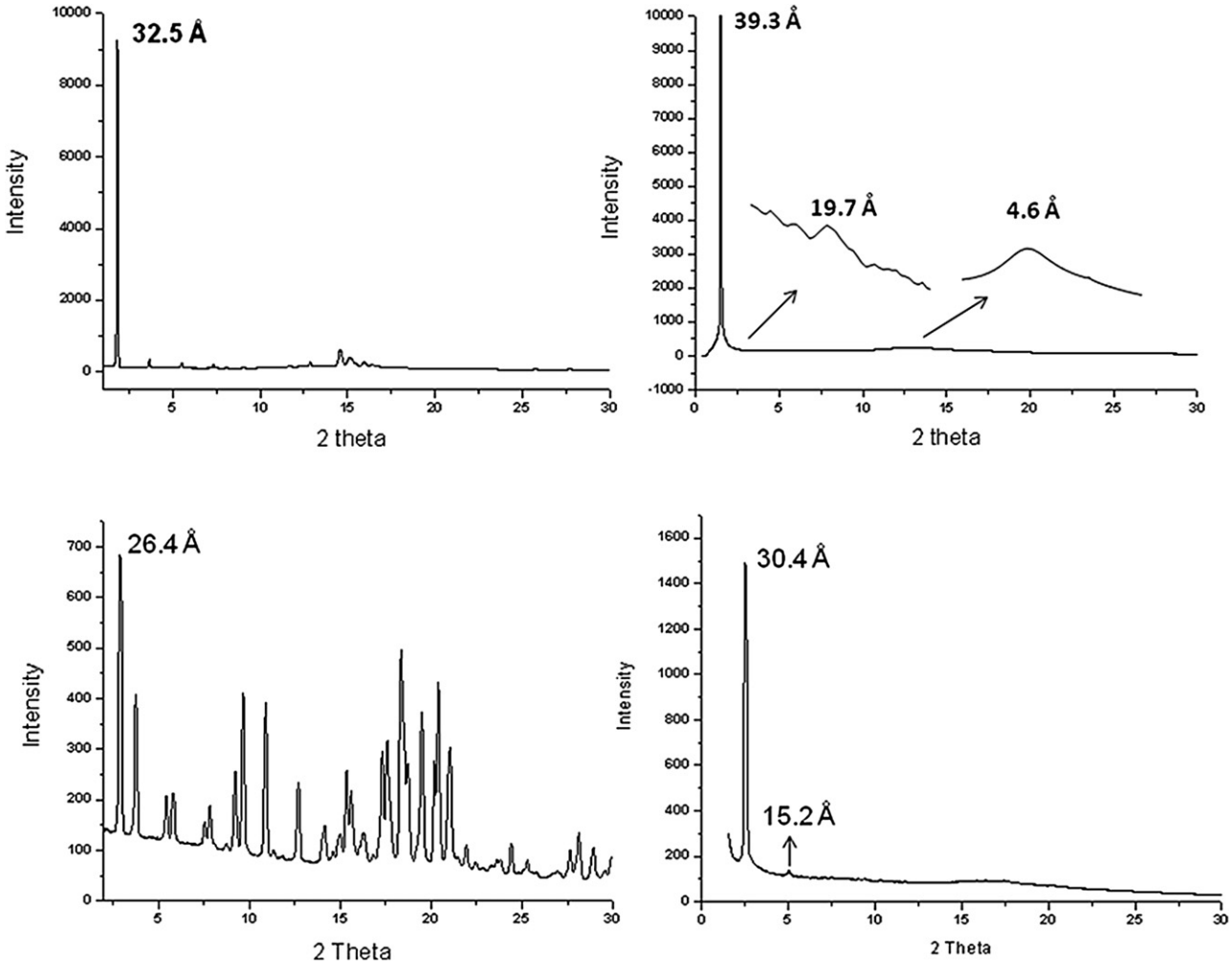


**Figure 8.** The powder X-ray diffraction plots for compounds. Top: **1a** ($n$=14) at 25.0 °C (left) and at 125.0 °C (right); bottom: **2a**/Pd ($n$=12) at 25.0 °C (left) and at 196.0 °C (right).

DSC analysis, all compounds **3a** were not mesogenic, and a phase transition from crystal-to-isotropic state was only observed at 243.1 ($n$=8)–222.1 °C ($n$=16). All compounds **3a** were also slightly decomposed above their clearing temperatures. In contrast, all compounds **3b** exhibited monotropic behavior. The clearing temperatures were drastically lower that those of compounds **3a**, which might be attributed to the structural effect. The temperature range of mesophases was quite short, ca. 4.80 ($n$=8)–17.3 °C ($n$=12). A too strong intermolecular H-bonding induced by two hydroxyl groups in compounds **3a** destroyed the liquid crystallinity. On the other hand, a weakening of H-bond interaction by only one hydroxyl group in compounds **3b** reached a well-balanced force needed to form the mesophases.

### 2.4. Variable-temperature powder XRD diffraction data

The mesophase structures for two compounds **1a** ($n$=14), **2a** (Pd, $n$=12) were also confirmed by use of variable-temperature powder XRD experiments. For compound **1a** ($n$=14) at $T$=125.0 °C a diffraction pattern with one strong peak, one weak peak and one very broad peat with a $d$-spacing of ca. ~39.3 Å, ~19.7 Å, and ~4.59 Å was observed (Fig. 8). The first two diffraction peaks

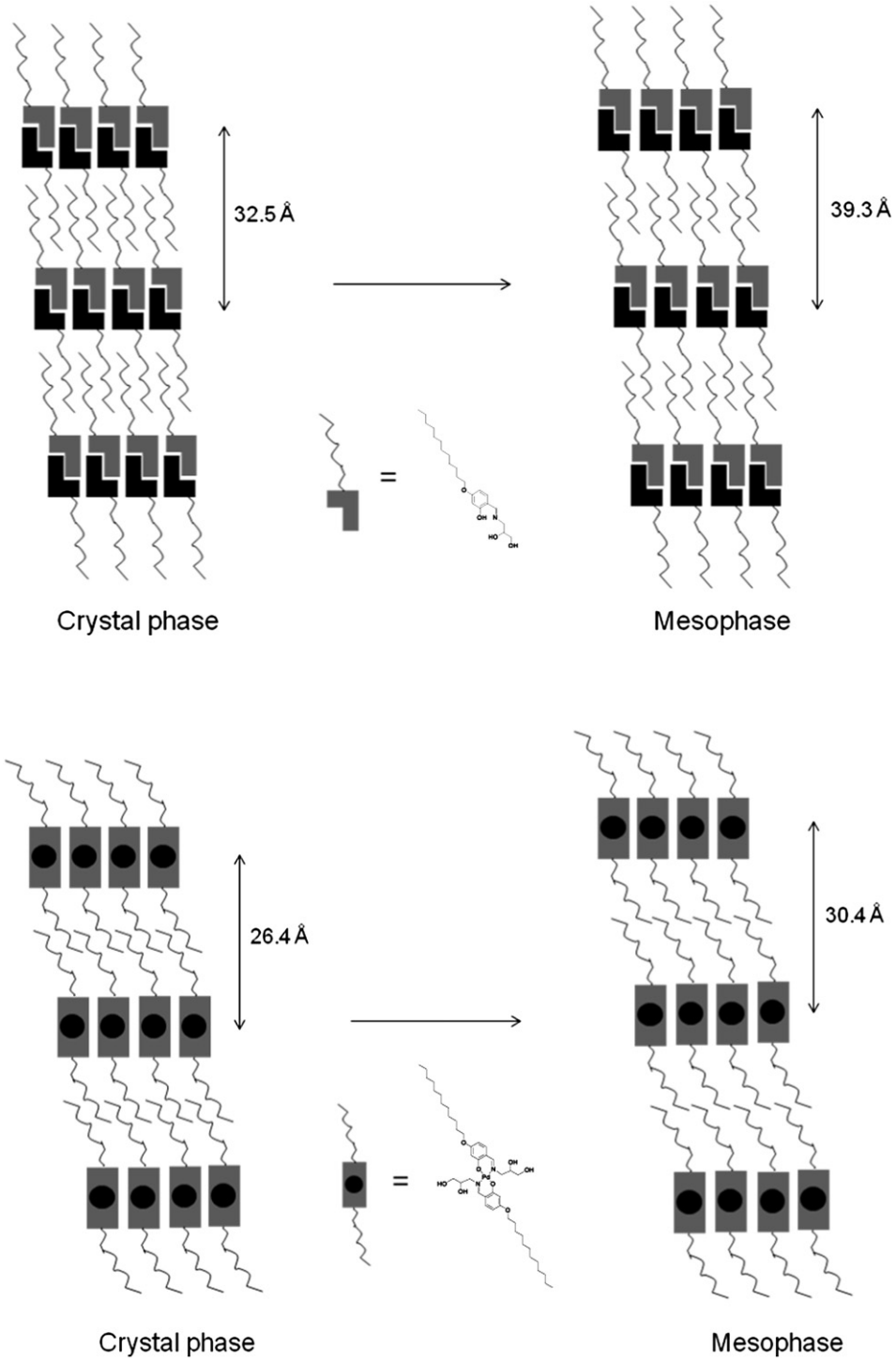


**Figure 9.** The schematic diagram showing the molecular arrangements proposed for compounds **1a** (top) and Pd complexes **2a** (bottom) both in Cr and SmA phase.

corresponded to a layer structure, assigned as 001 and 002 indices. The very broad weak of $d$~4.59 Å at wide angle region was due to halo diffraction. This diffraction pattern was typically characteristic of layer structures observed for a SmA phase. The layer $d$-spacing of 39.3 Å (**1a**; $n$=14) is much larger than the monomeric molecular length of~25.0 Å, a distance calculated for a fully extended molecule by MM2 model. However, it is much closer to the dimeric molecular length of~45.0 Å (**1a**; $n$=14), indicating that the formation of a smectic phase was induced or/and formed by a H-bonded dimeric structure with all alkoxy chains partially interdigitated.

XRD diffractions for palladium complex **2a** ($n$=12) both at 196.0 °C at 25.0 °C were also obtained. At 196.0 °C, a strong and a very weak diffraction peak at $d$=30.4 Å and $d$=15.2 Å assigned as 001 was observed. This diffraction pattern also confirmed the SmA phases. This $d$-spacing was close to the molecular length of 31.3 Å, obtained from single crystallographic data of complex **2a** ($n$=8) with four methylene moieties $(CH_2)_4$ on both sides added for complex **2a** ($n$=12). A molecular arrangement in the mesophase was therefore proposed in Figure 9.

## 3. Conclusions

Two series of new Schiff bases **1a**, **1b** and their palladium, vanadyl, and copper complexes **2**, **3** were prepared and their mesomorphic properties investigated to demonstrate the possible effect of induced H-bonds. Single crystallographic analysis of palladium complexes **2a** ($n$=8) confirmed the single crystal and molecular crystal structures. A dimeric structure with a better aspect ratio was induced by intermolecular H-bond, which led to the formation and facilitation of mesophases in compounds **2a**. All compounds **1** exhibited smectic A phases, in contrast, all metal complexes **2**, **3** formed smectic A and/or smectic X phases. Pd and VO complexes **2a**, **2b** exhibited similar mesomorphic behavior. The presence of a hydroxyl group at $C_{17}$- and $C_{18}$-position of Schiff imines played a significant role in forming the mesomorphic properties. Both palladium complexes **2a**, **2b** were mesogenic. However, compounds **2a** with two hydroxyl-OH groups attached on $C_{17}$ and $C_{18}$ have a higher clearing temperature than those of compounds **2a** with only one hydroxyl group attached on $C_{18}$, indicating a stronger intermolecular interaction in **2a**.

## 4. Experimental section

### 4.1. General

3-Amino-1,2-propanediol alcohol and 2,4-dihydroxybenzaldedyde were purchased from Acros used as received. The $^1H$ and $^{13}C$ NMR spectra were measured on a BUKER 300 UltraShield™ operated at 300 MHz with $CDCl_3$-$d_1$ as solvent with tetramethylsilane as the reference. DSC thermographs were carried out on a Mettler DSC 1 Star System. All phase transitions are determined by a scan rate of 10.0 °C/min. Optical polarized microscope was carried out on Zeiss Axioplan 2 equipped with a hot stage system of Mettler FP90/FP82HT. Elemental analysis for carbon, hydrogen, and nitrogen (Table 6) were conducted at Instrumentation Center, National Taiwan University on a Heraeus CHN–O-Rapid elemental analyzer. The powder X-ray diffraction data were collected from the Wiggler-A beam line of the National Synchrotron Radiation Research Center. The electrochemical experiment (CV) was carried out with a CHI 627C electrochemistry workstation (CHI, USA). A conventional three-electrode electrochemical system was used for the electrochemical experiment; this consisted of a working electrode, a platinum wire auxiliary electrode and a saturated Ag/AgCl reference electrode.

**Table 6**
Elemental analysis[a] of compounds **1**–**3**

| Compounds | C (%) | H (%) |
|---|---|---|
| **1a** ($n$=8) | 66.83 (66.84) | 9.10 (9.04) |
| **1a** ($n$=10) | 68.31 (68.34) | 9.54 (9.46) |
| **1a** ($n$=12) | 69.52 (69.62) | 9.85 (9.83) |
| **1a** ($n$=14) | 70.83 (70.72) | 10.23 (10.14) |
| **1a** ($n$=16) | 71.53 (71.68) | 10.40 (10.41) |
| **2a**–Pd ($n$=8) | 57.54 (57.55) | 7.51 (7.51) |
| **2a**–Pd ($n$=10) | 59.51 (59.23) | 7.98 (7.99) |
| **2a**–Pd ($n$=12) | 61.05 (61.20) | 8.38 (8.40) |
| **2a**–Pd ($n$=14) | 62.65 (62.69) | 8.87 (8.77) |
| **2a**–Pd ($n$=16) | 63.89 (64.01) | 9.08 (9.09) |
| **2b**–Pd ($n$=8) | 60.33 (60.12) | 8.01 (7.85) |
| **2b**–Pd ($n$=12) | 63.72 (63.56) | 8.82 (8.73) |
| **2b**–Pd ($n$=14) | 64.73 (64.95) | 9.00 (9.08) |
| **2b**–Pd ($n$=16) | 66.11 (66.18) | 9.36 (9.40) |
| **3a** ($n$=8) | 56.14 (56.16) | 7.06 (7.07) |
| **3a** ($n$=12) | 60.01 (59.91) | 8.10 (8.00) |
| **3a** ($n$=16) | 62.81 (62.81) | 8.72 (8.78) |
| **3b** ($n$=8) | 58.48 (58.59) | 7.45 (7.38) |
| **3b** ($n$=12) | 61.90 (62.16) | 8.30 (8.28) |
| **3b** ($n$=16) | 64.40 (64.90) | 8.86 (9.00) |

[a] With calculated values in parentheses.

### 4.2. X-ray crystallography

X-ray diffraction data were collected at 150 (2) K on a Nonius Kappa CCD X-ray diffractometer unit using graphite-monochromated Mo Kα radiation ($\lambda$=0.71073 Å) from crystals mounted on glass fibers and quickly coated in epoxy resin. Cell parameters were retrieved and refined using *DENZO-SMN* software on all observed reflections. Data reduction was performed with the *DENZO-SMN* software. The program package *SHELXTL* was used for space group determination, structure solution, and refinement. Refinement was performed against $F^2$ by weighted full-matrix least-square, and empirical absorption correction (SADABS) were applied. H atoms were placed at calculated positions using suitable riding models with isotropic displacement parameters derived from their carrier atoms. Crystal data, selected bond distances, and angles are provided in Tables 1 and 2.

*4.2.1. 4-Dodecyloxy-2-hydroxybenzaldehyde (n=12).* White solid, yield 40%. $^1H$ NMR (300 MHz, $CDCl_3$): $\delta$ 0.86 (t, $-CH_3$, 3H, $J$=6.80 Hz), 1.24–1.43 (m, $-CH_2$, 18H), 1.74–1.84 (m, $-OCH_2CH_2$, 2H), 3.97 (t, $-OCH_2$, 2H, $J$=6.58 Hz), 6.38 (S, Ar–H, 1H), 6.49 (dd, Ar–H, 1H, $J$=2.10 Hz), 6.50 (dd, Ar–H, 1H, $J$=2.15 Hz), 6.49 (dd, Ar–H, 1H, $J$=2.10 Hz), 7.38 (d, Ar–H, 1H, $J$=8.50 Hz), 9.67 (s, –CHO, 1H), 11.45 (s, Ar–OH, 1H). $^{13}C$ NMR (75 MHz, $CDCl_3$): $\delta$ 14.12, 22.70, 25.93, 25.98, 26.06, 28.20, 28.79, 28.94, 29.32, 29.36, 29.46, 29.55, 29.56, 29.59, 29.64, 31.93, 32.87, 33.99, 68.61, 101.06, 108.76, 115.02, 135.17, 164.55, 166.47, 194.25.

*4.2.2. 4-Hexadecyloxy-2-hydroxybenzaldehyde (n=16).* White solid, yield 45%. $^1H$ NMR (300 MHz, $CDCl_3$): $\delta$ 0.86 (t, $-CH_3$, 3H, $J$=6.38 Hz), 1.23–1.58 (m, $-CH_2$, 26H), 1.70–1.81 (m, $-OCH_2CH_2$, 2H), 3.98 (t, $-OCH_2$, 2H, $J$=6.53 Hz), 6.48 (dd, Ar–H, 1H, $J$=2.30 Hz), 6.52 (dd, Ar–H, 1H, $J$=2.15 Hz), 6.48 (dd, Ar–H, 1H, $J$=2.30 Hz), 7.39 (d, Ar–H, 1H, $J$=8.62 Hz), 9.68 (s, –CHO, 1H), 11.46 (s, Ar–OH, 1H). $^{13}C$ NMR (75 MHz, $CDCl_3$): $\delta$ 14.10, 22.68, 25.90, 28.90, 29.29, 29.51, 29.55, 29.65, 29.67, 31.91, 68.60, 101.03, 108.78, 114.99, 135.18, 164.51, 166.46, 194.28.

*4.2.3. 3-[(2-Hydroxy-4-dodecyloxybenzylidene)amino]propane-1,2-diol (**1a**; n=12).* The mixture of 4-dodecyloxy-2-hydroxybenzaldehyde (1.0 g, 2.63 mmol) dissolved in 5.0 mL of dried THF was added 3-amino-1,2-propanediol (0.25 g, 2.77 mmol) dissolved in 10 mL of absolute ethanol. The solution was refluxed for 3 h under nitrogen atmosphere. The solids were collected, and the

products, isolated as bright yellow solids were obtained after recrystallization from ether or hexane/THF at ice bath temperature. Yield 89%. $^1$H NMR (300 MHz, $CDCl_3$): $\delta$ 0.86 (t, $-CH_3$, 3H, $J$=6.9 Hz), 1.24–1.45 (m, $-CH_2$, 18H), 1.70–1.80 (m, $-OCH_2CH_2$, 2H), 3.55–3.79 (m, $-CH_2NC$, $-CH_2OH$, 4H), 3.93 (t, $-OCH_2$, 2H, $J$=6.6 Hz), 3.96–4.04 (m, −CHOH, 1H), 6.36 (b, Ar−H, 2H), 7.06 (d, Ar−H, 1H, $J$=9.3 Hz), 8.11 (s, −NCH, 1H). $^{13}$C NMR (75 MHz, $CDCl_3$): $\delta$ 14.10, 22.68, 25.98, 29.06, 29.34, 29.57, 31.91, 59.41, 64.55, 68.16, 71.32, 101.99, 107.24, 111.67, 133.13, 164.20, 165.57.

*4.2.4. 3-[(2-Hydroxy-4-octyloxybenzylidene)amino]propane-1,2-diol (**1a**; n=8).* Bright yellow solid, yield 86%. $^1$H NMR (300 MHz, $CDCl_3$): $\delta$ 0.86 (t, $-CH_3$, 3H, $J$=6.9 Hz), 1.26–1.46 (m, $-CH_2$, 10H), 1.71–1.76 (m, $-OCH_2CH_2$, 2H), 3.50–3.74 (m, $-CH_2NC$, $-CH_2OH$, 4H), 3.93 (t, $-OCH_2$, 2H, $J$=6.6 Hz), 3.96–4.03 (m, −CHOH, 1H), 6.28 (b, Ar−H, 2H), 7.02 (d, Ar−H, 1H, $J$=9.3 Hz), 8.02 (s, -NCH, 1H). $^{13}$C NMR (75 MHz, $CDCl_3$): $\delta$ 14.08, 22.64, 26.00, 29.06, 29.21, 29.33, 31.80, 58.76, 64.53, 68.15, 71.25, 102.15, 107.28, 111.46, 133.34, 164.50, 165.27.

*4.2.5. 3-[(2-Hydroxy-4-decyloxybenzylidene)amino]propane-1,2-diol (**1a**; n=10).* Bright yellow solid, yield 91%. $^1$H NMR (300 MHz, $CDCl_3$): $\delta$ 0.86 (t, $-CH_3$, 3H, $J$=6.9 Hz), 1.25–1.46 (m, $-CH_2$, 14H), 1.72–1.76 (m, $-OCH_2CH_2$, 2H), 3.51–3.75 (m, $-CH_2NC$, $-CH_2OH$, 4H,), 3.94 (t, $-OCH_2$, 2H, $J$=6.0 Hz), 3.96–4.01 (m, −CHOH, 1H), 6.29 (b, Ar−H, 2H), 7.03(d, Ar−H, 1H, $J$=8.4 Hz), 8.05 (s, −NCH, 1H). $^{13}$C NMR (75 MHz, $CDCl_3$): $\delta$ 14.08, 22.65, 25.98, 29.05, 29.30, 29.37, 31.87, 57.92, 64.46, 68.13, 71.14, 102.26, 107.26, 111.26, 133.51, 164.40, 165.01.

*4.2.6. 3-[(2-Hydroxy-4-tetradecyloxybenzylidene)amino]propane-1,2-diol (**1a**; n=14).* Bright yellow solid, yield 87%. $^1$H NMR (300 MHz, $CDCl_3$): $\delta$ 0.86 (t, $-CH_3$, 3H, $J$=6.9 Hz), 1.24–1.46 (m, $-CH_2$, 22H), 1.72–1.77 (m, $-OCH_2CH_2$, 2H), 3.53–3.79 (m, $-CH_2NC$, $-CH_2OH$, 4H,), 3.95 (t, $-OCH_2$, 2H, $J$=6.6 Hz), 3.98–4.00 (m, −CHOH, 1H), 6.35 (b, Ar−H, 2H), 7.07(d, Ar−H, 1H, $J$=9.0 Hz), 8.13 (s, −NCH, 1H). $^{13}$C NMR (75 MHz, $CDCl_3$): $\delta$ 14.11, 22.68, 25.97, 29.06, 29.35, 29.65, 31.91, 60.08, 64.54, 68.16, 71.37, 101.85, 107.20, 111.85, 132.98, 164.53, 165.85.

*4.2.7. 3-[(2-Hydroxy-4-hexadecyloxybenzylidene)amino]propane-1,2-diol (**1a**; n=16).* Bright yellow solid, yield 90%. $^1$H NMR (300 MHz, $CDCl_3$): $\delta$ 0.85 (t, $-CH_3$, 3H, $J$=6.9 Hz), 1.23–1.45 (m, $-CH_2$, 26H), 1.72–1.76 (m, $-OCH_2CH_2$, 2H), 3.53–3.79 (m, $-CH_2NC$, $-CH_2OH$, 4H), 3.92 (t, $-OCH_2$, 2H, $J$=6.3 Hz), 3.97–4.03 (m, −CHOH, 1H), 6.34 (b, Ar−H, 2H), 7.08 (d, Ar−H, 1H, $J$=9.3 Hz), 8.14 (s, −NCH, 1H). $^{13}$C NMR (75 MHz, $CDCl_3$): $\delta$ 14.09, 22.67, 25.97, 29.06, 29.34, 29.65, 31.91, 60.34, 64.54, 68.16, 71.41, 101.80, 107.18, 111.93, 132.91, 163.72, 165.98.

*4.2.8. N-(3-Hydroxypropyl)-4-dodecyloxysalicylaldimine (**1b**; n=12).* The mixture of 4-dodecyloxy-2-hydroxybenzaldehyde (1.0 g, 2.63 mmol) and 3-amino- propan-1-ol (0.21 g, 2.77 mmol) was refluxed in 15 mL of absolute ethanol for 3 h. The solution was cooled and the solids were collected. The products, isolated as yellow needle crystals were obtained after recrystallization from hexane. Yield 85%. $^1$H NMR (300 MHz, $CDCl_3$): $\delta$ 0.86 (t, $-CH_3$, 3H, $J$=6.9 Hz), 1.27–1.78 (m, $-CH_2$, 18H), 1.94 (m, $-OCH_2CH_2$, 2H), 3.64 (t, $-CH_2NC$, 2H, $J$=6.6 Hz), 3.74 (t, $-CH_2OH$, 2H, $J$=6.0 Hz), 3.93 (t, $-OCH_2$, 2H, $J$=6.6 Hz), 6.31 (d, Ar−H, 1H, $J$=2.10 Hz), 6.34 (s, Ar−H, 1H), 7.05 (d, Ar−H, 1H, $J$=8.4 Hz), 8.12 (s, -NCH, 1H). $^{13}$C NMR (75 MHz, $CDCl_3$): $\delta$ 14.11, 22.64, 25.96, 29.03, 29.31, 29.52, 29.61, 31.54, 33.27, 53.14, 59.69, 68.03, 101.90, 106.80, 111.60, 132.70, 163.80, 168.10.

*4.2.9. N-(3-Hydroxypropyl)-4-octyloxysalicylaldimine (**1b**; n=8).* Yellow needle crystal, yield 85%. $^1$H NMR (300 MHz, $CDCl_3$): $\delta$ 0.87 (t, $-CH_3$, 3H, $J$=6.9 Hz), 1.27–1.79 (m, $-CH_2$, 10H), 1.95 (m, $-OCH_2CH_2$, 2H), 3.61 (t, $-CH_2NC$, 2H, $J$=6.6 Hz), 3.74 (t, $-CH_2OH$, 2H, $J$=6.0 Hz), 3.92 (t, $-OCH_2$, 2H, $J$=6.6 Hz), 6.3 (d, Ar−H, 1H, $J$=2.10 Hz), 6.34 (s, Ar−H, 1H), 7.05 (d, Ar−H, 1H, $J$=8.4 Hz), 8.11(s, -NCH, 1H). $^{13}$C NMR (75 MHz, $CDCl_3$): $\delta$ 14.11, 22.64, 25.96, 29.03, 29.52, 31.54, 31.88, 33.27, 53.15, 59.69, 68.04, 101.90, 106.80, 111.60, 132.70, 163.90, 168.10.

*4.2.10. N-(3-Hydroxypropyl)-4-hexadecyloxysalicylaldimine (**1b**; n=16).* Yellow needle crystal, yield 82%. $^1$H NMR (300 MHz, $CDCl_3$): $\delta$ 0.86 (t, $-CH_3$, 3H, $J$=6.9 Hz), 1.28–1.79 (m, $-CH_2$, 26H), 1.93 (m, $-OCH_2CH_2$, 2H), 3.64 (t, $-CH_2NC$, 2H, $J$=6.6 Hz), 3.75 (t, $-CH_2OH$, 2H, $J$=6.0 Hz), 3.93 (t, $-OCH_2$, 2H, $J$=6.6 Hz), 6.31 (d, Ar−H, 1H, $J$=2.40 Hz), 6.35 (s, Ar−H, 1H), 7.06 (d, Ar−H, 1H, $J$=8.7 Hz), 8.13 (s, -NCH, 1H). $^{13}$C NMR (75 MHz, $CDCl_3$): $\delta$ 14.09, 22.65, 25.97, 29.03, 29.32, 29.52, 29.57, 29.61, 29.63, 29.65, 31.54, 31.88, 33.27, 53.14, 59.69, 68.0, 101.90, 106.80, 111.60, 132.70, 163.80, 168.20.

### 4.3. Palladium and vanadyl complex of 3-[(2-hydroxy-4-dodecyloxybenzylidene)amino] propane-1,2-diol (2a; *n*=12)

The mixture of 3-[(2-hydroxy-4-dodecyloxybenzylidene) amino]propane-1,2-diol (0.50 g, 0.58 mmol) and palladium (II) acetate (0.065 g, 0.29 mmol) or $VOSO_4$ (0.047 g, 0.29 mmol) was stirred in 20 mL of THF for 6 h. The solids were collected and the products, isolated as yellow solids for vanadyl complexes or light gray-green for palladium complexes were obtained after recrystallization from THF/methanol at ice bath temperature. Yield 70–76%. Vanadyl complexes were only slightly soluble in THF, and it was not stable in THF. The color changed to red in a few minutes.

### 4.4. Copper complex of 3-[(2-hydroxy-4-dodecyloxybenzylidene)amino]propane-1,2-diol (3a; *n*=12)

The mixture of 3-[(2-hydroxy-4-dodecyloxybenzylidene) amino]propane-1,2-diol (0.50 g, 0.58 mmol) and copper(II) acetate (0.11 g, 0.58 mmol) was refluxed in THF for 6 h. The solids were collected, and the products, isolated as green powder were obtained after recrystallization from THF/methanol at ice bath temperature. Yield 80%.

*4.4.1. Palladium complex of N-(3-hydroxypropyl)-4-dodecyloxysalicylaldimine (**2b**; n=12).* The mixture of *N*-(3-hydroxypropyl)-4-dodecyloxysalicylaldimine (0.50 g, 1.38 mmol) dissolved $CHCl_3$ was added palladium(II) acetate (0.15 g, 0.69 mmol) dissolved in 10.0 mL of ethanol. The mixture was refluxed for 8 h. The solution was concentrated and the products, isolated as yellow solids were obtained after recrystallization from hexane/dichloromethane. Yield 75%.

*4.4.2. Copper complex of N-(3-hydroxypropyl)-4-dodecyloxysalicylaldimine (**3b**; n=12).* The mixture of *N*-(3-hydroxypropyl)-4-dodecyloxysalicylaldimine (0.50 g, 1.38 mmol) dissolved in 5.0 mL of $CHCl_3$ was added copper(II) acetate (0.25 g, 1.38 mmol) dissolved in 10 mL of ethanol. The mixture was refluxed for 1 h. The solution was concentrated and the product, isolated as brown solids was obtained after recrystallization from ethyl acetate/methanol. Yield 86%.

### Acknowledgements

We thank the National Science Council of Taiwan, ROC (NSC98-2815-C-008-021-M & NSC98-2752-M-008-010-PAE) and Industrial Technology Research Institute of Taiwan, ROC (ITRI-99-B-069351-A-A-5130) in generous support of this work.

## References and notes


1. (a) Coco, S.; Cordovilla, C.; Domínguez, C.; Donnio, B.; Espinet, P.; Guillon, D. *Chem. Mater.* **2009**, *21*, 3282–3289; (b) Lavigueur, C.; Foster, E. J.; Williams, V. E. *J. Am. Chem. Soc.* **2008**, *130*, 11791–11800; (c) Kutsumizu, S.; Mori, H.; Fukatami, M.; Naito, S.; Sakajiri, K.; Saito, K. *Chem. Mater.* **2008**, *20*, 3675–3687; (d) Barberá, J.; Puig, L.; Romero, P.; Serrano, J. L.; Sierra, T. *J. Am. Chem. Soc.* **2006**, *128*, 4487–4492; (e) Barberá, J.; Puig, L.; Romero, P.; Serrano, J. L.; Sierra, T. *J. Am. Chem. Soc.* **2005**, *127*, 458–464; (f) Yagai, S.; Nakajima, T.; Kishikawa, K.; Kohmoto, S.; Karatsu, T.; Kitamra, A. *J. Am. Chem. Soc.* **2005**, *127*, 11134–11139; (g) Chen, B.; Baumeister, U.; Diele, S.; Das, M. K.; Zeng, X.; Ungar, G.; Tschierske, C. *J. Am. Chem. Soc.* **2004**, *126*, 8608–8609; (h) Prehm, M.; Diele, S.; Das, M.; Tschierske, C. *J. Am. Chem. Soc.* **2003**, *125*, 614–615.
2. (a) Miao, J.; Zhu, L. *Chem. Mater.* **2010**, *22*, 197–206; (b) Vera, F.; Serrano, J. L.; Sierra, T. *Chem. Soc. Rev.* **2009**, *38*, 781–796; (c) Giménez, R.; Elduque, A.; López, J. A.; Barberá, J.; Cavero, E.; Lantero, I.; Oro, L. A.; Serrano, J. L. *Inorg. Chem.* **2006**, *45*, 10363–10370; (d) Massiot, P.; Impéror-Clerc, M.; Veber, M.; Deschenaux, M. *Chem. Mater.* **2005**, *17*, 1946–1951; (e) Ziessel, R.; Pickaert, G.; Camerel, F.; Donnio, B.; Guillon, D.; Cesario, M.; Prange, T. *J. Am. Chem. Soc.* **2004**, *126*, 12403–12413.
3. Wang, Y. J.; Song, J. H.; Lin, Y. S.; Lin, C.; Sheu, H. S.; Lee, G. H.; Lai, C. K. *Chem. Commun.* **2006**, 4912–4914.
4. *Tetrahedron* **2010**. doi:10.1016/j.tet.2010.03.04
5. (a) Bilgin-Eran, B.; Yűrőr, C.; Tschierske, C.; Prehm, M.; Baumeister, U. *J. Mater. Chem.* **2007**, *17*, 2319–2328; (b) Bilgin-Eran, B.; Tschierske, C.; Diele, S.; Baumeister, U. *J. Mater. Chem.* **2006**, *16*, 1136–1144; (c) Murillas, D. L.; Piñol, R.; Ros, B.; Serrano, J. L.; Sierra, T.; Fuente, M. R. *J. Mater. Chem.* **2004**, *14*, 1117–1127; (d) Hegmann, T.; Kain, J.; Diele, S.; Schubert, B.; Bőgela, H.; Tschierske, C. *J. Mater. Chem.* **2003**, *13*, 991–1003; (e) Díez, L.; Espinet, P.; Miguela, J. A.; Rosb, M. B. *J. Mater. Chem.* **2002**, *12*, 3694–3698.
6. Rezvani, Z.; Divband, B.; Abbasi, A. R.; Nejati, K. *Polyhedron* **2006**, *25*, 1915–1920.
7. (a) Lai, C. K.; Leu, Y. F. *J. Chin. Chem. Soc.* **1997**, *44*, 89–91; (b) Lai, C. K.; Lu, M. Y.; Lin, F. J. *Liq. Cryst.* **1997**, *23*, 313–315; (c) Lai, C. K.; Lin, R.; Lu, M. Y.; Kao, K. C. *Dalton Trans.* **1998**, 1857–1862.
8. (a) Mohebbi, S.; Bakhshi, B. *J. Coord. Chem.* **2008**, *61*, 2615–2628; (b) Krishnamurthy, S. S.; Soundarajan, S. *J. Inorg. Nucl. Chem.* **1966**, *28*, 1689–1692; (c) Kasahara, R.; Tsuchimoto, M.; Ohba, S.; Nakajima, K.; Ishida, H.; Kojima, M. *Inorg. Chem.* **1996**, *35*, 7661–7665; (d) Zhao, H. Y.; Xing, Y. H.; Cao, Y. Z.; Li, Z. P.; Wei, D. M.; Zeng, X. Q.; Ge, M. F. *J. Mol. Struct.* **2009**, *938*, 54–64; (e) Chang, C. J.; Labinger, J. A.; Gray, H. R. *Inorg. Chem.* **1997**, *36*, 5927–5930; (f) Ooi, S.; Nishizawa, M.; Matsumoto, K.; Kuroya, H.; Saito, K. *Bull. Chem. Soc. Jpn.* **1979**, *52*, 452–457; (g) Mohan, M.; Stephen, M. H.; Butcher, R. J.; Jasinski, J. P.; Carano, C. J. *Inorg. Chem.* **1992**, *31*, 2029–2034.
9. (a) Lintvedt, R. L.; Ranger, G.; Schoenfelner, B. A. *Inorg. Chem.* **1984**, *23*, 688–695; (b) Zehetmair, J. K.; Lintvedt, R. L. *Inorg. Chem.* **1990**, *29*, 2201–2204; (c) Wang, M. Y.; Xu, X. Y.; Yang, F.; Zhang, S. Y.; Yang, X. J. *J. Appl. Electrochem.* **2008**, *38*, 1269–1274.